Adaptive Fourier decomposition based ECG denoising

Ze Wang, Feng Wan, Chi Man Wong, Liming Zhang

www.elsevier.com/locate/cbm

PII: S0010-4825(16)30210-4
DOI: http://dx.doi.org/10.1016/j.compbiomed.2016.08.013
Reference: CBM2480

To appear in: *Computers in Biology and Medicine*

Received date: 1 April 2016
Revised date: 13 August 2016
Accepted date: 18 August 2016

Cite this article as: Ze Wang, Feng Wan, Chi Man Wong and Liming Zhang, Adaptive Fourier decomposition based ECG denoising, *Computers in Biolog and Medicine,* http://dx.doi.org/10.1016/j.compbiomed.2016.08.013

Adaptive Fourier decomposition based ECG denoising

Ze Wang[a], Feng Wan[a,*], Chi Man Wong[a], Liming Zhang[b]

[a]*Department of Electrical and Computer Engineering, Faculty of Science and Technology, University of Macau, Taipa, Macau*
[b]*Department of Computer and Information Science, Faculty of Science and Technology, University of Macau, Taipa, Macau*

Abstract

A novel ECG denoising method is proposed based on the adaptive Fourier decomposition (AFD). The AFD decomposes a signal according to its energy distribution, thereby making this algorithm suitable for separating pure ECG signal and noise with overlapping frequency ranges but different energy distributions. A stop criterion for the iterative decomposition process in the AFD is calculated on the basis of the estimated signal-to-noise ratio (SNR) of the noisy signal. The proposed AFD-based method is validated by the synthetic ECG signal using an ECG model and also real ECG signals from the MIT-BIH Arrhythmia Database both with additive Gaussian white noise. Simulation results of the proposed method show better performance on the denoising and the QRS detection in comparing with major ECG denoising schemes based on the wavelet transform, the Stockwell transform, the empirical mode decomposition, and the ensemble empirical mode decomposition.

Keywords: Adaptive Fourier decomposition, Electrocardiogram (ECG), Signal denoising, Gaussian noise

1. Introduction

The electrocardiogram (ECG) signal is a weak and noise-prone electrical interpretation of the heart activity [1]. Noise is the unwanted components generated due to non-cardiac reasons, which acts as a source of error in the signal analysis [2]. Therefore, a suitable signal denoising method must be applied for ECG signals to determine the correct heart condition. The Fourier transform is one conventional signal denoising technique. However, due to the nonlinear and non-stationary properties of the ECG signals, this method is limited in the capability to the ECG denoising [3]. To overcome this shortcoming, several new approaches have been proposed [1–10]. Among them, the wavelet transform (WT) based methods are widely used because of their abilities to remove Gaussian noise [3–6]. However, the performance of the WT-based denoising methods depends on their selected mother wavelets [9]. Since mother wavelets used in the WT are independent of the processed signals, a suitable mother wavelet that always provides favorable filtered results is difficult to be found [4, 9]. Moreover, the WT requires various decomposition levels to represent ECG signals. The unsuitable threshold selection of these decomposition levels may oscillate the reconstructed ECG signal or reduce the amplitude of the ECG waveform [5]. Recently, the synchrosqueezed wavelet transform (SWT) and the multiple signal classification-empirical wavelet transform (MUSIC-EWT) were proposed to overcome these drawbacks of the WT [9, 11]. In the SWT, the synchrosqueezing operation reallocates the energy of wavelet coefficients to enhance frequency localization, which makes the SWT be able to isolate main frequency components from noise [10, 12]. The MUSIC-EWT introduces the adaptability to the WT by building a bank of wavelet filters based on the pseudospectrum of the time-series signal determined via the MUSIC method, which can provide an efficient time-frequency representation for nonlinear and non-stationary noisy signals [9]. Except the SWT and the MUSIC-EWT, the Stockwell transform (S-transform), the empirical mode decomposition (EMD) and extension versions of the EMD, like the ensemble EMD (EEMD), were proposed to overcome these shortcoming of the WT. The S-transform also allows adaption of the time resolution depending on the frequency components of the signal [12]. In recent literatures, Das and Ari et al. [1, 13] show that the ECG denoising performance of the S-transform is better than that of the WT. However, a critical step in the real implementation of the S-transform is the fast FT (FFT), which indicates that the S-transform inherits some drawbacks of the conventional Fourier decomposition, such as the low energy convergence rate and the trade-off between the time resolution and the frequency resolution [1, 13]. For the signal denoising methods based on the EMD and its extension versions, the key ideas are same. They primarily filter out the intrinsic mode functions (IMFs) that contain the largest amount of noise, and then reconstruct the denoising result using reminders [2, 7, 8]. Since the EMD is based on the local characteristics of data, its decomposition components can be derived adaptively [14]. However, this method does not have an explicit mathematical explanation, thereby making its decomposition results difficult to understand and interpret. Moreover, the analytic phase functions of IMFs are not monotone in some cases [15]. In other words, a physically meaningful analytic instantaneous frequency of IMFs cannot be defined in general, which will affect the time-frequency analysis of IMFs [14, 16–18].

To overcome afore-mentioned limitations, the adaptive Fourier decomposition (AFD) method is proposed by Qian et al.

*Corresponding author. Tel.: +853 8822 4473; fax: +853 8822 2426.
Email address: fwan@umac.mo (Feng Wan)

[17, 19, 20]. The AFD is a generalization of the conventional Fourier decomposition method combined with the greedy algorithm to expand processed signals into series mono-components (MCs) that only contain non-negative analytic phase derivatives [19, 21]. Compared with the WT and the S-transform, the AFD generates its basis adaptively based on processed signals to achieve fast energy convergence. Moreover, in contrast to the EMD, the AFD has a rigorous mathematical foundation [17, 19]. Our previous work in [22] shows that in most cases the denoising performance of the AFD is better than that of the Butterworth low-pass filter, the WT and the EMD for the muscle and electrode motion artifacts. However, it does not explain how to determine the stop criterion of the AFD which is critical in the ECG denoising. Moreover, in [22], only the signal-to-noise ratio (SNR) is applied to evaluate the denoising performance, which cannot depict clearly the quality of the biology-related information enhanced by the AFD.

In this paper, an AFD-based ECG denoising method is proposed on the basis of the assumption that the energy of the pure ECG signal is higher than that of noise in the noisy signal. A stop criterion of the AFD is calculated using the estimated SNR of the noisy signal to maximize the SNR of the denoised result. The proposed method is validated using an ECG model and the real ECG signals in the MIT-BIH Arrhythmia Database [23–25]. This paper concerns only the additive Gaussian white noise, a basic and common noise model for many random processes in nature, such as the noise due to poor channel conditions [1, 26]. The muscle noise, which occurs probably during ECG acquisition and may not be able to be modeled as the Gaussian white noise [1, 27], has been already studied using the AFD method for denoising in our previous work [22]. Moreover, the ECG denoising performance in this paper is evaluated by not only the SNR and the mean square error (MSE) showing the noise reduction results but also the sensitivity and the positive predictivity of the R-peak detection giving the quality of the biology-related information preserved by the denoised ECG signals based on the AFD. The statistical analysis reveals that the proposed method has the best performance compared to the WT, S-transform, EMD and EEMD.

This paper is organized as follows: Section 2 presents the mathematical foundation of the AFD, Section 3 shows the proposed AFD-based ECG denoising method, Section 4 illustrates simulation results of the proposed method, Section 5 provides a formal discussion including separate results and comparisons between the proposed method and the ECG denoising methods based on the WT, S-transform, EMD and EEMD, finally the conclusion is given in Section 6.

2. Mathematical foundation of the AFD

The AFD involves the adaptive decomposition of a given analytic signal $G(t)$ that is in H^2 space into a series of MCs $s_n(t)$ and a standard remainder $R_N(t)$ as shown in

$$G(t) = \sum_{k=0}^{\infty} c_k e^{jkt} = \sum_{n=1}^{N} s_n(t) + R_N(t), \quad \sum_{k=0}^{\infty} |c_k|^2 < \infty. \tag{1}$$

where $\mathbb{D} = \{z \in \mathbb{C} : |z| < 1\}$ and $\mathbb{C}$ is the complex plane [19]. The AFD uses the rational orthogonal system $\{B_n\}_{n=1}^{\infty}$ as its basis functions where

$$B_n(e^{jt}) = \frac{\sqrt{1-|a_n|^2}}{1-\overline{a}_n e^{jt}} \prod_{k=1}^{n-1} \frac{e^{jt}-a_k}{1-\overline{a}_k e^{jt}}, \tag{2}$$

$a_n \in \mathbb{D}$, and $n = 1, 2, \cdots$ [19]. It should be noted that the characteristics of $B_n(e^{jt})$ are only depended on the array of a_n [28]. The main process of the AFD is to find suitable a_n array that can make the energy convergence rate high.

The AFD sequentially extracts MCs from high-energy components to low-energy components. To find the energy relationship easily, the reduced remainders G_n are defined as follows using their corresponding standard remainders R_{n-1} [19]:

$$G_n(e^{jt}) = R_{n-1}(e^{jt}) \prod_{l=1}^{n-1} \frac{1-\overline{a}_l e^{jt}}{e^{jt}-a_l}. \tag{3}$$

Then, (1) can be expressed as follows using the reduced remainders G_n:

$$G(t) = \sum_{n=1}^{N} \langle G_n, e_{\{a_n\}} \rangle B_n(e^{jt}) + G_{N+1}(e^{jt}) \prod_{n=1}^{N} \frac{e^{jt}-a_n}{1-\overline{a}_n e^{jt}} \tag{4}$$

where $e_{\{a_n\}}(e^{jt})$ is called the evaluator at a_n that can be considered as a dictionary consisting the following elementary functions [19]:

$$e_{\{a_n\}}(e^{jt}) = \frac{\sqrt{1-|a_n|^2}}{1-\overline{a}_n e^{jt}}. \tag{5}$$

According to (4), the energy of $G(t)$ can be calculated as follows [19]:

$$\|G(t)\|^2 = \sum_{n=1}^{N} \left|\langle G_n, e_{\{a_n\}} \rangle\right|^2 + \left\|G_{N+1}(e^{jt})\right\|^2. \tag{6}$$

To achieve a high energy convergence rate, the energy of the standard remainder $\left\|G_{N+1}(e^{jt})\right\|^2$ in every decomposition level must be kept at minimum. Therefore, the maximal projection principle (MPP) shown in (7) is applied to find a_n [19].

$$a_n = \arg\max \left\{ \left|\langle G_n, e_{\{a_n\}} \rangle\right|^2 : a_n \in \mathbb{D} \right\} \tag{7}$$

The AFD largely differs from the conventional Fourier decomposition methods. Instead of merely depending on frequency analysis, signals are decomposed by the AFD based on their energy distribution, which makes this method suitable for separating two parts with overlapping frequency ranges and separate energy concentrations.

3. Signal denoising method based on the AFD

Before applying the AFD, the mean value of the measured noisy signal $s(t)$ is removed to avoid the effect of the DC offset. Then, the noisy signal should be projected to H^2 space using the Hilbert transform defined as [29]

$$\mathcal{H}\{s(t)\} = \frac{1}{\pi} \int_{-\infty}^{\infty} s(t) \frac{1}{t-\tau} d\tau. \tag{8}$$

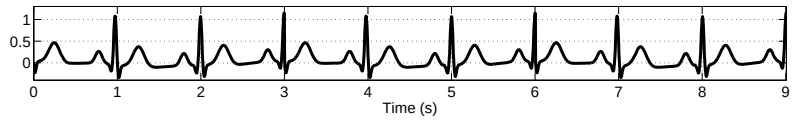

(a) Synthetic ECG signal based on the ECG model

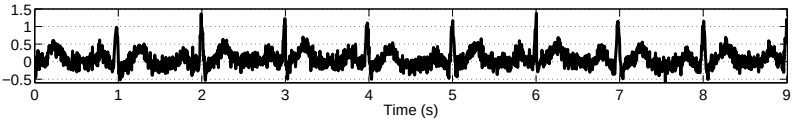

(b) Noisy ECG signal with additive Gaussian white noise at the 5 dB SNR level

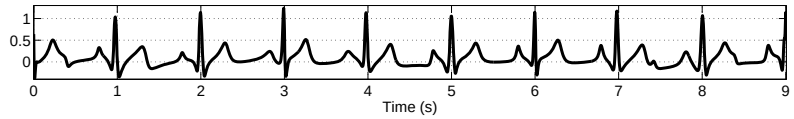

(c) Denoised signal based on the proposed method

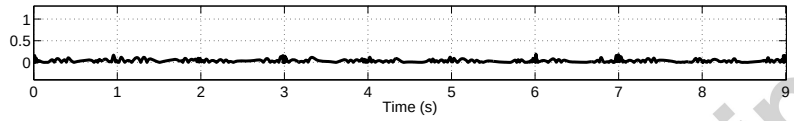

(d) Absolute error between the pure and denoised signals

Figure 1: ECG denoising performance of the AFD-based ECG denoising method for the synthetic ECG signal.

Considering the concept of the analytic signal [30], the analytic representation of the noisy signal can be described as

$$G(t) = s(t) + j\,\mathcal{H}\{s(t)\} \tag{9}$$

which is applied as the input of the AFD. Suppose that the noisy signal is expressed by

$$s(t) = h(t) + w(t) \tag{10}$$

where $h(t)$ denotes the pure signal to be recovered, and $w(t)$ denotes the independent noise which energy is smaller than that of $h(t)$, then the AFD will extract MCs of the pure signal first during the decomposition. Therefore, such MCs in the first N decomposition levels can be selected to approximate the pure signal. Based on the decomposition components of $G(t)$, the reconstructed ECG signal $\hat{h}(t)$ can be expressed as

$$\hat{h}(t) = \mathrm{Re}\left\{\sum_{n=1}^{N} \langle G_n, e_{\{a_n\}}\rangle\, B_n(e^{jt})\right\}. \tag{11}$$

The key problem is to determine a suitable maximum decomposition level N adaptively. To solve this problem, a stop criterion of the AFD is proposed based on the estimated SNR of the noisy signal. Since the denoising aims to make the MSE defined as

$$\mathrm{MSE} = L^{-1} E\left\|\hat{h} - h\right\|^2 \tag{12}$$

as small as possible where L denotes the total data length [31, 32], the reconstructed ECG signal at the suitable decomposition level N should be able to minimize

$$\frac{\|s(t)\|^2}{\left\|\hat{h}(t)\right\|^2} - \left(1 + \frac{1}{10^{\mathrm{SNR}_e/10}}\right) \tag{13}$$

where SNR_e defined as

$$\mathrm{SNR}_e = 10 \log \frac{\|h(t)\|^2}{\|w(t)\|^2} \tag{14}$$

denotes the estimated SNR of the noisy signal. According to (6) and (11), the energy of the reconstructed ECG signal can be represented as

$$\left\|\hat{h}(t)\right\|^2 = \frac{1}{2}\sum_{n=1}^{N} \left|\langle G_n, e_{\{a_n\}}\rangle\right|^2. \tag{15}$$

Then, combining (13) and (15), the suitable maximum decomposition level N can be determined by solving

$$\min_{N>1, N\in\mathbb{Z}} \left\{\left| \frac{\|s(t)\|^2}{\frac{1}{2}\sum_{n=1}^{N}\left|\langle G_n, e_{\{a_n\}}\rangle\right|^2} - \left(1 + \frac{1}{10^{\mathrm{SNR}_e/10}}\right)\right|\right\}. \tag{16}$$

Since the standard remainder $R_N(t)$ in (1) satisfies

$$\|R_N(t)\| \le \frac{M}{\sqrt{N}} \tag{17}$$

where M is a constant that is related to the energy of the decomposed signal [33], the energy of the standard remainder $R_N(t)$ decreases as the decomposition level N increases. In other words, the energy ratio of the noisy signal to the reconstructed signal decreases monotonically when the decomposition level N increases, which means that (16) only has one optimization solution. Therefore, (16) can be used as the stop criterion of the iterative process of the AFD in the ECG denoising process. The objective function value in (16) is evaluated at each decomposition level. At first decomposition levels, the objective function

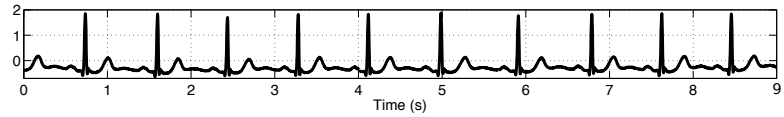

(a) Original ECG signal (MIT-BIH record 103)

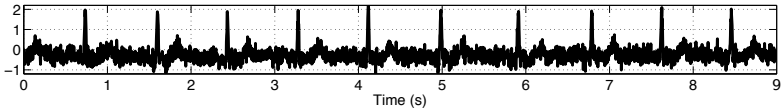

(b) Noisy ECG signal with additive Gaussian white noise at the 5 dB SNR level

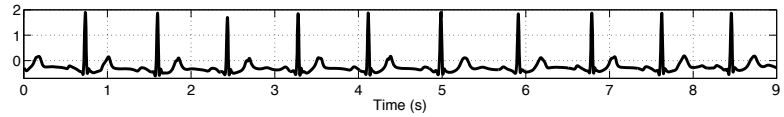

(c) Denoised signal based on the proposed method

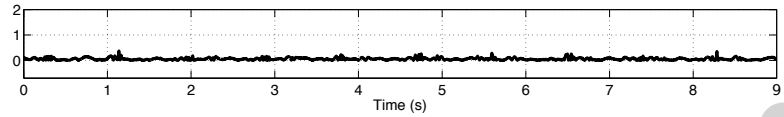

(d) Absolute error between the original and denoised signals

Figure 2: ECG denoising performance of the AFD-based ECG denoising method for the real ECG signal.

Algorithm 1 Computational process of the AFD-based ECG denoising method.

Input: $s(t)$: noisy ECG signal; SNR_e: estimated SNR of $s(t)$.

$s(t) \leftarrow s(t) - \mathrm{mean}\{s(t)\}$;

$G(t) \leftarrow s(t) + \mathcal{H}\{s(t)\}$

Initialize $a_1 = 0$, $N = 1$, $G_1(t) = G(t)$, $e_{\{a_1\}} = 1$, and $B_1 = 1$;

repeat

$G_{N+1} \leftarrow \left(G_N(t) - \langle G_N, e_{\{a_N\}}\rangle\, e_{\{a_N\}}\right) \frac{1-\overline{a}_N e^{jt}}{e^{jt}-a_N}$;

$e_{\{a_{N+1}\}} \leftarrow \frac{\sqrt{1-|a_{N+1}|^2}}{1-\overline{a}_{N+1}e^{jt}}$;

$a_{N+1} \leftarrow \arg\max \left\{ \left| \langle G_{N+1}, e_{\{a_{N+1}\}}\rangle \right|^2 : a_{N+1} \in \mathbb{D} \right\}$;

$B_{N+1} \leftarrow \frac{\sqrt{1-|a_{N+1}|^2}}{1-\overline{a}_{N+1}e^{jt}} \frac{e^{jt}-a_N}{\sqrt{1-|a_N|^2}} B_N$;

$N \leftarrow N + 1$;

$OFV \leftarrow \left| \frac{\|s(t)\|^2}{\frac{1}{2}\sum_{n=1}^{N} \left|\langle G_n, e_{\{a_n\}}\rangle\right|^2} - \left(1 + \frac{1}{10^{\mathrm{SNR}_e/10}}\right) \right|$;

until OFV achieves its minimum value

$\hat{h} \leftarrow \mathrm{Re}\left\{ \sum_{n=1}^{N} \langle G_n, e_{\{a_n\}}\rangle\, B_n \right\}$;

Output: $\hat{h}$: reconstructed filtered result; N: final decomposition level.

values will decrease. When the objective function achieves its minimum point, the decomposition iteration should be stopped. The filtered result can be reconstructed by using all extracted MCs based on (11).

In each decomposition level, one value in the a_n array is determined from the dictionary based on the MPP. Although the dictionary of a_n can be adaptively generated according to the processed signals [21], the optimization problem shown in (7) cannot be solved efficiently using the exhaustive searching method. Therefore, to improve the computational efficiency of the MPP implementation, the Nelder-Mead algorithm is applied in the process of searching a_n [34]. The main computational process of the proposed method is shown in Algorithm 1.

4. Simulation results

Simulations are carried out in the MATLAB using two types of ECG signals: the synthetic ECG signal based on an ECG model proposed in [23] and real ECG signals from the MIT-BIH Arrhythmia Database. The signal generated by the ECG model is applied to verify the signal denoising principle shown in Section 3, while real ECG signals are used to verify the ECG denoising performance of the proposed method. The performance of the proposed method is evaluated based on the SNR and the MSE. In the following evaluations, the SNR of the reconstructed ECG signal is calculated by

$$\mathrm{SNR} = 10 \log \frac{\sum_{t=0}^{L-1} h(t)^2}{\sum_{t=0}^{L-1} \hat{w}(t)^2} \tag{18}$$

where $h(t)$ is the synthetic ECG signal or the real ECG signal, and $\hat{w}(t)$ is the noise of the reconstructed signal which is estimated by

$$\hat{w}(t) = \hat{h}(t) - h(t) \tag{19}$$

where $\hat{h}(t)$ is the reconstructed signal. The MSE is calculated by

$$\mathrm{MSE} = \frac{\sum_{t=0}^{L-1} \left[\hat{h}(t) - h(t)\right]^2}{L}. \tag{20}$$

Because absolute error is small, signals' magnitudes are increased up to 200 times their original values to illustrate error clearly when calculating MSE. To evaluate the quality of the biology-related information preserved in the denoised ECG

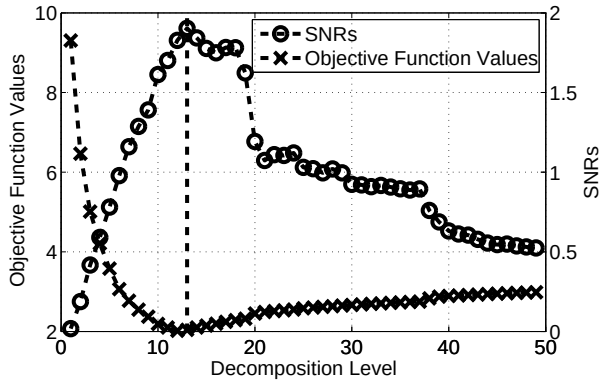

Figure 3: SNRs of the reconstructed signals and the objective function values of (16) in the first 50 decomposition levels.

signal, R-peak detection test is performed for the denoised ECG signals. The R-peak detection algorithm is implemented based on the Pan-Tompkins algorithm [35]. The sensitivity *Se* and the positive predictivity *+P* are considered to evaluate the QRS complex detection results, which can be calculated by

$$Se = \frac{TP}{TP + FN} \tag{21}$$

and

$$+P = \frac{TP}{TP + FP} \tag{22}$$

where *TP*, *FN* and *FP* denotes the number of true positive, false negative and false positive, respectively [1].

4.1. Simulation results based on the synthetic ECG signal

The synthetic ECG signal is based on a nonlinear dynamical ECG model that is proposed in [23]. The sampling frequency and heart rate are set to 256Hz and 60 beats per minute, respectively. Figure 1(a) shows the synthetic ECG signal. The additive Gaussian white noise is added to the signal resulting in a noisy signal at the 5 dB SNR level as shown in Figure 1(b). Figure 1(c) illustrates the filtered signal generated by the proposed method. On the basis of the proposed stop criterion, the filtered signal is reconstructed by the first 13 MCs obtained from the AFD. Figure 1(d) shows the absolute differences between the pure synthetic ECG signal and the filtered signal. Although unexpected sharp peaks are observed around the P-waves and T-waves, the absolute error is small. In other words, these peaks do not affect the amplitudes of these complexes.

To verify the selection of the maximum decomposition level, the SNRs of the reconstructed signals and the objective function values of (16) in the first 50 decomposition levels are shown in Figure 3. The cross and circle dash lines represent the objective function values and SNRs of the reconstructed signals, respectively. The curve of the objective function values contains only one minimum point at the decomposition level $N = 13$ which is indicated by a vertical dash line. The curve of SNRs achieves its maximum value at the same decomposition level. These observations satisfy the description in section 3 and confirm that the proposed stop criterion is suitable for the ECG denoising process of AFD.

4.2. Simulation results based on real ECG signals

Real ECG records from the MIT-BIH Arrhythmia Database are applied to verify ECG denoising performance of the proposed method. Figure 2(a) illustrates the nine-second signal of the record 103. Figure 2(b) shows the record 103 signal with additive Gaussian white noise at the 5 dB SNR level. Figure 2(c) shows the filtered signal generated by the proposed method, while Figure 2(d) shows the absolute differences between the original signal and the filtered signal. It can be seen that the reconstructed signal can represent the original ECG signal with a very small error. Figure 4 shows the statistical results of the denoising performance of the proposed method for all records in the database where "Input SNR" denotes the SNRs of noisy signals, and "Output SNR", "Output MSE", "Output +P" and "Output Se" denote the SNRs, MSE, *+P* and *Se* of the filtered signals, respectively. The additive Gaussian white noise is added to generate noisy signals at the SNR levels from 0 dB to 10 dB. To remove effects of the random process in the noise generation step, 50 independent simulations and their average performance are performed for each case. Figure 4(a) illustrates the box plot for the MSE of filtered signals. Since signals' magnitudes are increased up to 200 times their original values to illustrate error clearly when calculating MSE, values of MSE seems very large. However, comparing to signals' magnitudes, MSE of filtered signals for most records is small. In addition, the MSE of the filtered signal increases along with the decreasing SNR of the noisy signal. Figure 4(b) shows that the SNRs of filtered signals with different noise levels, which indicates that SNRs of filtered signals are always higher than that of noisy signals, which shows that the proposed method is able to denoise real ECG signals. Moreover, the SNR of the filtered signal decreases along with the increasing noise level of the noisy signal. Figure 4(c) and Figure 4(d) show R-peak detection results. It can be seen that the sensitivities and positive predictivities of the filtered signals are all close to 1, which indicates that those ECG signals denoised by the proposed method can achieve a very good QRS complex detection performance. Although the proposed method shows good performance in most records, outliers in Figure 4 denotes that denoising results for some records are worse than others, which will be discussed in Section 5. To illustrate the advancements of the proposed method, the simulation results based on the WT, the S-transform, the EMD and the EEMD proposed by the literature are compared with that based on the proposed method.

Table 1 and Table 2 compare the ECG denoising performance of the proposed method and the WT-based method. Since selected mother wavelets and types of thresholds are two key parameters in the WT-based denoising methods, the ECG denoising performance of the proposed method is compared with different parameter selections. Table 1 compares ECG denoising performance of the proposed method and the WT-based methods with different mother wavelets (DB4 and DB6). Results of the WT with different mother wavelets in Table 1 are taken from [4] in which the additive Gaussian white noise is added to the record 103 ECG signal resulting 4 different SNR levels. The results of WT with different types of thresholds in Table 2 are taken from [1] in which additive Gaussian white noise is

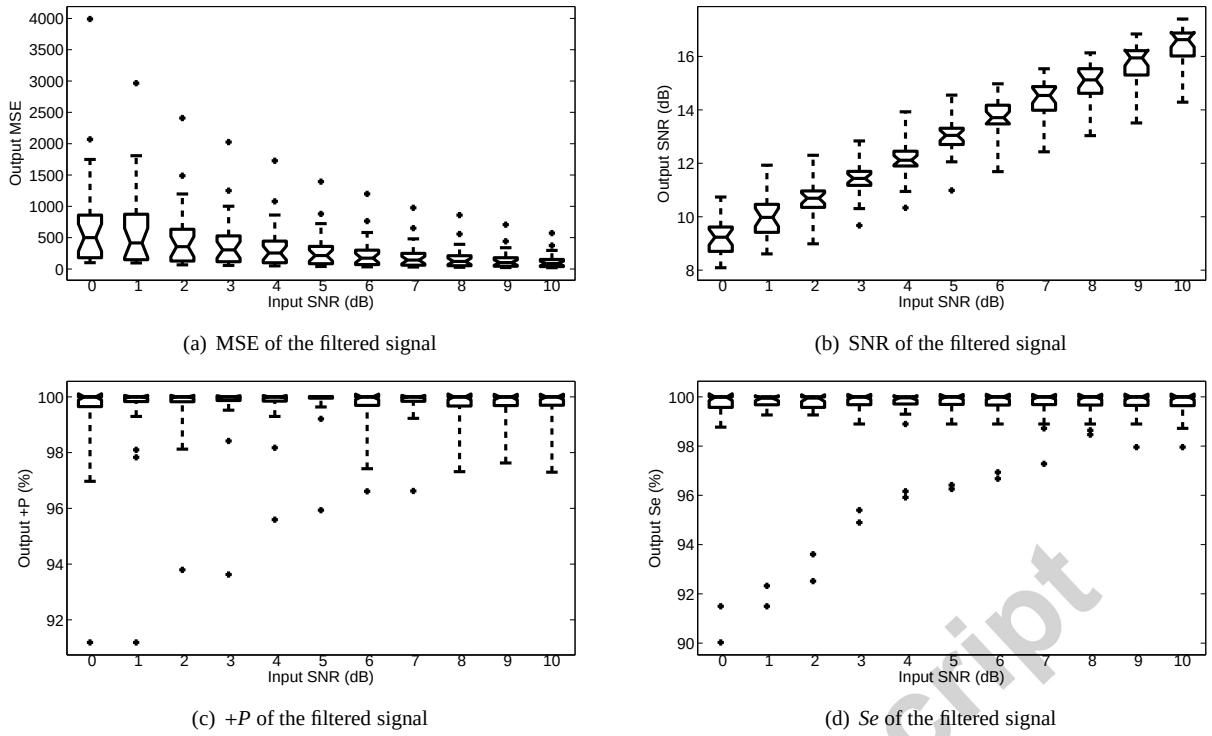

(a) MSE of the filtered signal

(b) SNR of the filtered signal

(c) $+P$ of the filtered signal

(d) *Se* of the filtered signal

Figure 4: Box plot of the ECG denoising performance for real ECG signals with different noisy levels.

Table 1: ECG denoising performance (SNR in dB) comparison between the filtered results based on the WT with different mother wavelets and the proposed method for the record 103 signal.

SNR of noisy signal (dB)	6.8	9.29	12.81	15.83
WT based on DB4	11.81	13.55	15.84	18.02
WT based on DB6	11.38	12.87	15.07	18.70
Proposed method	**14.52**	**16.35**	**18.70**	**20.52**

added to 10 different ECG records in the MIT-BIH Arrhythmia database resulting 3 different SNR levels where "WT-soft" and "WT-subband" denote the WT based on the soft threshold and the WT based on subband depended threshold, separately [1]. It can be seen that the WT-based methods fail to improve the signal quality in some cases, especially for those cases with low input SNR levels [1]. However, the proposed method always demonstrates better ECG denoising performance than the WT-based methods. Table 2 also shows the ECG denoising results of the S-transform-based method taken from [1]. It can be seen that the proposed method also provides higher filtered SNRs than the S-transform-based method. Table 3 shows the one-way-ANOVA-based statistical analysis of the comparison results presented in Table 2. Values of F are all very large, which indicates relatively more differences between groups. Since values of *sig* are all close to 0, such differences are significant.

Table 4 shows the comparison results of the R-peak detection based on the WT-soft, WT-subband, S-transform, and proposed method. The detection results of those methods based on the WT-soft, WT-subband, and S-transform are taken from [1] in which ECG denoising methods are applied to remove additive Gaussian white noise added to two ECG records selected from the MIT-BIH Arrhythmia Database resulting the 1.25 dB SNR level. It can be seen that, except the positive predictivity of the detection results of record 230, the detection sensitivity and positive predictivity of the proposed method are always the highest among those of other methods. Besides the R-peak, other major characteristic waves in the ECG, such as the T, P, Q, and S waves, are also crucial in the ECG signals but usually less intense than the R peak. Figure 5 illustrates the influence of the proposed method on these waves. In the noisy signal shown in Figure 5(b), T, P, Q, and S waves are difficult to identify, which would result in both false positive and false negative in the detection of these waves and also may generate false alarm for heart abnormality [8, 36]. From Figure 5(c), the T, P, Q, and S waves show significant peaks in the denoised ECG signal, which will benefit the subsequent detection and segmentation. In these characteristic waves, the QT interval reflects the time between the depolarization and repolarization of the heart ventricles, which is an important electrocardiographic parameter, often used to quantify the duration of ventricular repolarization [37]. To show how the proposed method can help to raise the accuracy of the QT detection, simulations are conducted to the ECG signals selected from the QT database of the Physionet

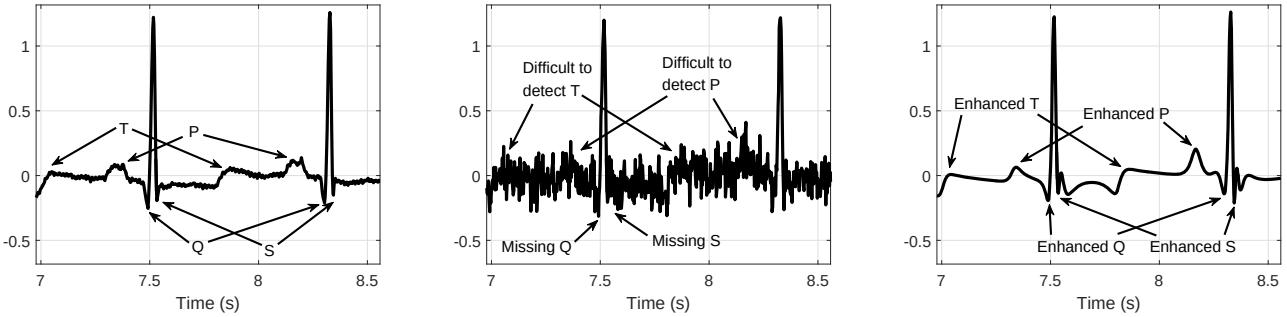

(a) Original ECG signal (b) Noisy ECG signal with additive Gaussian white noise at the 5dB SNR level (c) Denoised ECG signal using the proposed method

Figure 5: Denoised ECG signal obtained from the AFD-based ECG denoising method compared to the original and noisy ECG signals in two periods.

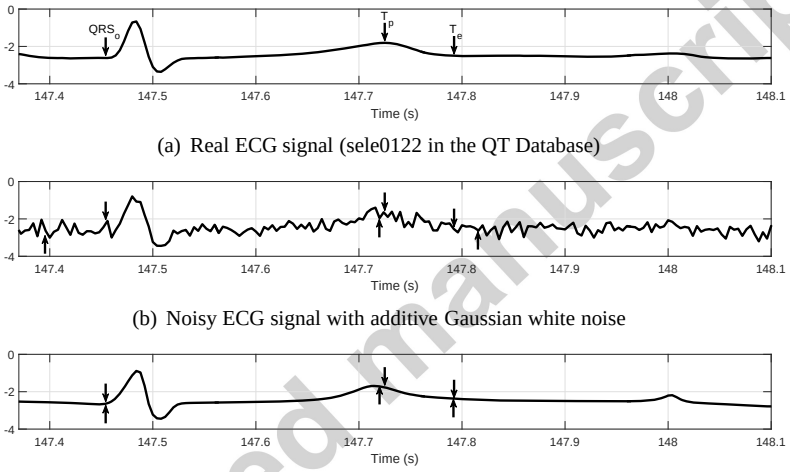

(a) Real ECG signal (sele0122 in the QT Database)

(b) Noisy ECG signal with additive Gaussian white noise

(c) Denoised ECG signal using the proposed method

Figure 6: Detection results of QRS$_o$, T$_p$ and T$_e$.

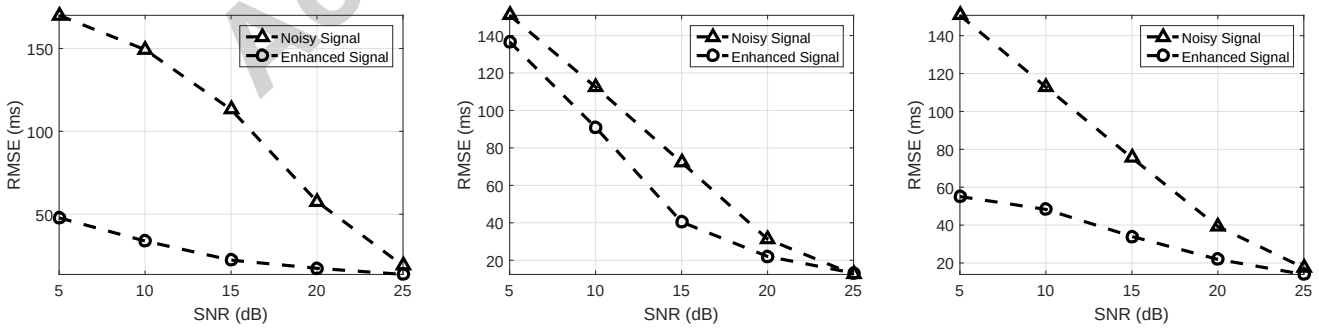

(a) QRS$_o$ (b) T$_p$ (c) T$_e$

Figure 7: RMSE of QRS$_o$, T$_p$ and T$_e$ determination in the noisy ECG signals at different SNR levels and denoised ECG signals using the proposed method.

Table 2: ECG denoising performance (SNR in dB) comparison between the filtered results based on the WT with different types of thresholds, S-transform, and proposed method.

Record No.		103	105	111	116	122	205	213	219	223	230
WT-soft method	0 dB	5.54	7.35	7.04	6.63	6.69	5.45	5.91	7.25	7.35	5.73
	1.25 dB	6.72	7.96	7.72	7.37	7.47	6.31	6.62	8.02	8.10	6.44
	5 dB	9.66	10.22	9.62	9.65	9.77	8.57	8.74	10.36	10.87	8.85
WT-subband method	0 dB	6.69	7.68	7.06	6.87	7.23	6.44	7.13	6.92	7.35	6.55
	1.25 dB	7.77	8.65	7.78	7.83	8.50	7.55	8.08	8.45	8.32	7.62
	5 dB	10.51	12.11	9.85	9.76	9.86	9.22	9.67	11.01	11.21	9.14
S-transform	0 dB	9.96	8.85	7.55	7.95	8.32	8.45	8.14	8.94	9.56	9.93
	1.25 dB	10.95	9.95	8.71	8.73	9.32	9.15	9.42	10.03	10.81	11.05
	5 dB	12.91	13.54	10.09	9.82	11.42	10.10	12.49	12.54	13.86	13.14
Proposed method	0 dB	**10.29**	**9.04**	**8.53**	**9.15**	**8.83**	**9.39**	**8.58**	**10.05**	**9.59**	**10.05**
	1.25 dB	**11.28**	**10.21**	**9.63**	**10.26**	**9.92**	**10.06**	**9.60**	**10.97**	**10.89**	**11.17**
	5 dB	**13.11**	**13.81**	**12.47**	**13.05**	**12.53**	**12.40**	**12.64**	**14.00**	**14.55**	**13.34**

Table 3: One-way ANOVA analysis of the denoising performance comparison between filtered results based on the WT with different types of thresholds, the S-transform, and the proposed method.

Input SNR level (dB)	Source of variation	Sum of squares	df	Mean squares	F	sig
0	Between groups	56.52	3	18.84	41.14	0.00
	Within groups	16.49	36	0.46		
	Total	73.01	39			
1.25	Between groups	64.37	3	21.46	47.06	0.00
	Within groups	16.41	36	0.46		
	Total	80.79	39			
5	Between groups	79.66	3	26.55	24.62	0.00
	Within groups	38.83	36	1.08		
	Total	118.48	39			

resources [25, 38]. These signals include the traces of healthy subjects, sel16483, sel16786, sel16795 as well as diseased subjects: sel808, sele0122 and sele0170 which are also selected in [37]. The real ECG signals are assumed contaminated with the additive Gaussian white noise at the SNR levels from 5 dB to 25 dB. The noisy signals and the denoised signals are analyzed for the QRS onset (QRS_o), the T wave peak (T_p) and the T wave end (T_e) determination. A robust method developed by Martinez et al. [39] is applied to the detection. For comparison, the detection is also performed on the original ECG signal. Figure 6 illustrates the denoising performance for one beat signal of sele0122. The arrows directed upwards show the detection results on the original real ECG signal. The arrows directed downwards show the detection results on the noisy signal and the denoised signal. Large errors of QRS_o and T_e determination, which occur when the detections are performed on the noisy signal, are precluded after the signal denoising. These visual results are confirmed in Figure 7 that illustrates the root mean squared errors (RMSE) of the respective characteristic point detections in the noisy signals and denoised signals. For the noisy signals, the high SNR level is required to determine the respective positions precisely. After the ECG denoising based on the proposed method, the precision of detections is significantly raised. Especially for the low SNR cases, such as 5 dB and 10 dB, the errors of QRS_o and T_e determination for the denoised signals are much lower than those for the noisy signals.

Table 5 compares the ECG denoising performance of the proposed method and those methods based on the EMD and the EEMD. The results of the EMD and the EEMD are taken from [7] in which the additive Gaussian white noise is added to 16 records of ECG signals from the MIT-BIH Arrhythmia Database resulting in the 10 dB SNR level. Although the filtered MSE of the proposed method is much higher than that of the EMD and EEMD for the record 203 signal, the proposed method can provide better ECG denoising performance than methods based on the EMD and EEMD most of time. The reason of the poor performance of the proposed method for the record 203 is discussed in the next section.

5. Discussion

The AFD decomposes signal to MCs based on its energy distribution, making it possible to separate the desired signal and the noise components with which have overlapping frequency ranges but different energy distributions. Accordingly, this paper proposes a novel approach based on the AFD for the ECG signal denoising. The stop criterion is selected to stop the AFD in order to maximize the SNR of the reconstructed signal. The ECG denoising performance is evaluated by not only the SNR and the MSE showing the noise reduction effect but also the sensitivity and the positive predictivity of the R-peak detection describing the enhanced quality of the biology-related information.

Tables 1, 2, 3 and 5 give the noise reduction performance of the proposed method. More specifically, Tables 1 and 2 show

Table 4: R-peak detection performance of noisy signals and denoised ECG signals using the WT-soft, WT-subband, S-transform, and proposed method.

Record No.	Noisy signal		WT-soft		WT-subband		S-transform		Proposed method	
	Se (%)	+P (%)	Se (%)	+P (%)	Se (%)	+P (%)	Se (%)	+P (%)	Se (%)	+P (%)
103	79.17	79.06	99.47	99.00	99.62	99.62	99.66	99.62	99.75	99.75
230	74.04	74.04	98.89	98.37	99.56	99.34	99.78	99.82	99.87	99.82

Table 5: ECG denoising performance (MSE) comparison between filtered results based on the EMD, the EEMD, and the proposed method with the noisy signal at the 10 dB SNR level.

Record No.	101	102	103	104	105	106	107	108	109	201	202	203	205	207	208	209
EMD	126.9	83.3	189.4	151.6	180.6	245.6	771.7	103.2	237.2	67.1	131.3	279.7	72.5	129.7	361.2	140.3
EEMD	97.4	60.0	147.0	109.5	128.1	192.5	574.9	76.9	179.7	38.6	76.3	**206.5**	55.0	99.9	232.0	103.3
Proposed method	**36.0**	**32.6**	**76.0**	**55.7**	**73.6**	**98.9**	**572.6**	**24.0**	**112.1**	**38.3**	**28.4**	321.3	**29.5**	**93.9**	**199.2**	**60.8**

a comparison on the denoising performances between the proposed method and the WT based methods with either DB4 or DB6 wavelets as well as either soft or subband based thresholds. It can be seen that the proposed method performs always better in comparison with the denoising results of the WT based methods taken from [1] and [4]. Table 2 also provides the comparison result between the proposed method and the S-transform based method proposed by Ari et al. [1], where it is found that our method offers a larger SNR improvement than the S-transform based method. One-way ANOVA analysis results for the comparison in Table 2 is given in Table 3, showing that the differences between the ECG denoising performances of the proposed method, the WT based methods with the soft and subband based thresholds, and the S-transform based method are significant. Moreover, the proposed method is also compared with the EMD and the EEMD based methods proposed by Chang et al. [7] and the comparison results are given in Table 5, indicating that the denoising performances of the proposed method are better than those of the EMD and EEMD based methods in most cases.

Figure 8 illustrates the statistical analysis results for Tables 1, 2 and 5 using the box plot representation. Particularly, the statistical evaluation for Table 5 is shown in Figure 8(e), where the four outliers indicate the EMD-based, the EEMD-based and the AFD-based simulation results of the record 107 and the AFD-based simulation result of the record 203, respectively. The poor performance of these records also can be found in Figure 4, which is mainly due to the low quality of the original signals (i.e., the records 107 and 203) and the denoising performance calculation. As an example, Figures 9(a) and 9(b) show a segment of the signal in three seconds from the record 103 at normal quality, and the record 203 at low quality, respectively. Comparatively, the original ECG signal in the record 203 already contains significant amount of noise and this noise cannot be ignored and should not be included in the pure ECG signal. Meanwhile, Table 5 uses the MSE index, treating such noise as a part of the pure ECG signal, which results in unfortunately an ineffective description of the denoising performance in some cases, such as for the records 107 and 203 which contain large noise. The true denoising performance of the proposed method can be observed from Figure 9(d), which shows the filtered results for the original signals with the additive Gaussian white noise added at the 10 dB SNR level as shown in Figure 9(c), using the proposed method with 10 dB as the estimated SNR. Furthermore, the true SNR of the noisy signal would be lower than 10 dB as the noise contained in the original signal should be also considered for estimating the SNR of the noisy signal. Accordingly, with the estimated SNR adjusted to 8.5 dB, Figure 9(e) shows a better filtered result for the proposed method, where it is found that both the noise in the original signal and the artificial noise are almost filtered out.

In addition to the noise reduction results, the denoising performance is also evaluated by the detection results of the R-peak, QRS_o, T_p and T_e shown in Table 4 as well as Figures 5, 6 and 7. Table 4 shows a comparison on the R-peak detection results on the denoised signals using the proposed method, the WT based method and the S-transform based method. The detection results on the denoised signals using the WT and the S-transform are from [1]. Comparatively, the proposed method can provide higher sensitivities and positive predictivities. Moreover, the RMSE results of the detections for QRS_o, T_p and T_e at the SNR levels from 5 dB to 25 dB is shown in Figure 7, where the RMSE results on the denoised signals using the proposed method are found lower than those on the noisy signals, and the detection accuracy can be improved at different noise levels.

6. Conclusions

This paper proposes an AFD-based ECG signal denoising algorithm that uses a stop criterion calculated by the estimated SNR of the noisy signal. The noise components are removed from the energy domain, thereby allowing the proposed method to separate the pure signal and noise with overlapping frequency ranges but different energy distributions. The stop criterion is calculated to maximize the SNR of the reconstructed signal. This criterion is then verified by an synthetic ECG signal based on an ECG model. The ECG denoising performance of the proposed method is evaluated using real ECG signals from the MIT-BIH Arrhythmia Database for different noise levels and is then compared with the performance of ECG denoising schemes based on the WT, the S-transform, the EMD, and

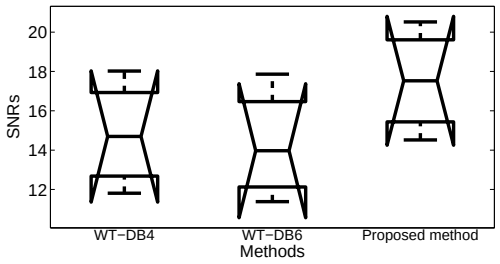

(a) Statistical evaluation of Table 1

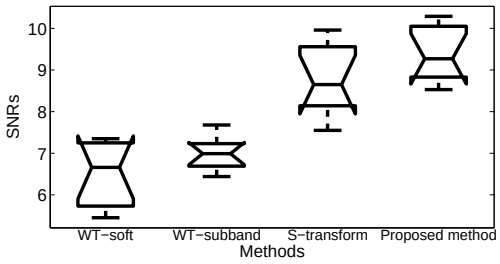

(b) Statistical evaluation of Table 2 for 0 dB SNR noise level

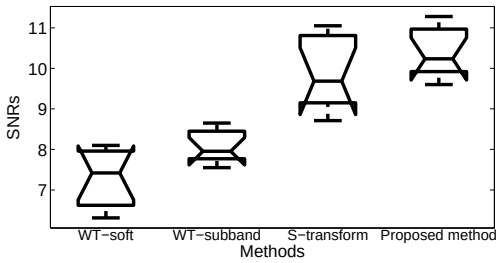

(c) Statistical evaluation of Table 2 for 1.25 dB SNR noise level

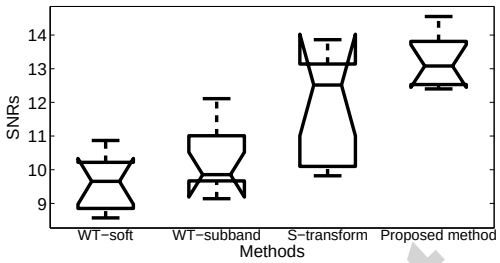

(d) Statistical evaluation of Table 2 for 5 dB SNR noise level

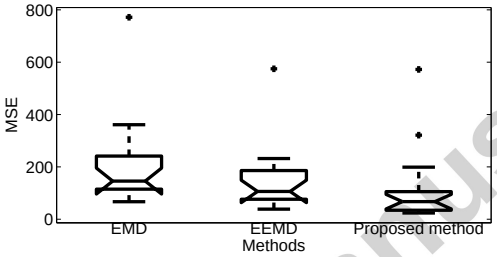

(e) Statistical evaluation of Table 5

Figure 8: Box plot based statistical evaluations of denoising performance comparisons shown in Table 1, 2 and 5.

the EEMD. The statistical analysis reveals that the proposed method outperforms the other methods, which indicates that the AFD is a promising tool for ECG denoising.

Acknowledgments

The authors would like to thank the anonymous reviewers and the editor in chief for their constructive and detailed comments that helped to very much improve the quality of this paper.

This work is supported in part by the Macau Science and Technology Development Fund under grants FDCT 036/2009/A and FDCT 055/2015/A2 and the University of Macau Research Committee under grants MYRG139(Y1-L2)-FST11-WF, MYRG079(Y1-L2)-FST12-VMI, MYRG069(Y1-L2)-FST13-WF, MYRG2014-00174-FST and MYRG2016-00240-FST.

References

[1] S. Ari, M. K. Das, A. Chacko, ECG signal enhancement using S-transform, Comput. Biol. Med. 43 (6) (2013) 649–660. doi:10.1016/j.compbiomed.2013.02.015.

[2] S. Pal, M. Mitra, Empirical mode decomposition based ECG enhancement and QRS detection, Comput. Biol. Med. 42 (1) (2012) 83–92. doi:10.1016/j.compbiomed.2011.10.012.

[3] M. Alfaouri, K. Daqrouq, ECG signal denoising by wavelet transform thresholding, Am. J. Appl. Sci. 5 (3) (2008) 276–281. doi:10.3844/ajassp.2008.276.281.

[4] E. Ercelebi, Electrocardiogram signals de-noising using lifting-based discrete wavelet transform, Comput. Biol. Med. 34 (6) (2004) 479–493. doi:10.1016/S0010-4825(03)00090-8.

[5] G. U. Reddy, M. Muralidhar, S. Varadarajan, ECG de-noising using improved thresholding based on wavelet transforms, Int. J. Comput. Sci. Netw. Security 9 (9) (2009) 221.

[6] M. Sakai, D. Wei, Separation of electrocardiographic and encephalographic components based on signal averaging and wavelet shrinkage techniques, Comput. Biol. Med. 39 (7) (2009) 620–629. doi:10.1016/j.compbiomed.2009.04.009.

[7] K. M. Chang, S. H. Liu, Gaussian noise filtering from ECG by Wiener filter and ensemble empirical mode decomposition, J. Signal Process. Sys. 64 (2) (2011) 249–264. doi:10.1007/s11265-009-0447-z.

[8] S. Agrawal, A. Gupta, Fractal and EMD based removal of baseline wander and powerline interference from ECG signals, Comput. Biol. Med. 43 (11) (2013) 1889–1899. doi:10.1016/j.compbiomed.2013.07.030.

[9] J. P. Amezquita-Sanchez, H. Adeli, A new MUSIC-empirical wavelet transform methodology for timefrequency analysis of noisy nonlinear and non-stationary signals, Digit. Signal Process. 45 (2015) 55–68. doi:10.1016/j.dsp.2015.06.013.

[10] J. P. Amezquita-Sanchez, H. Adeli, Synchrosqueezed wavelet transform-fractality model for locating, detecting, and quantifying damage in smart highrise building structures, Smart Mater. Struct. 24 (6) (2015) 065034. doi:10.1088/0964-1726/24/6/065034.

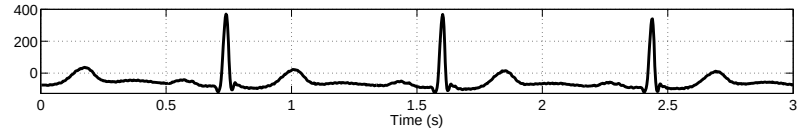

(a) Original ECG signal (MIT-BIH record 103)

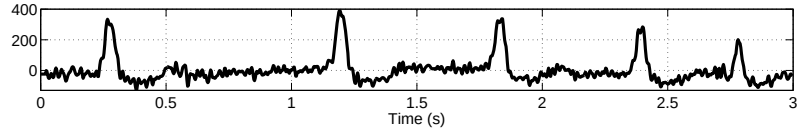

(b) Original ECG signal (MIT-BIH record 203)

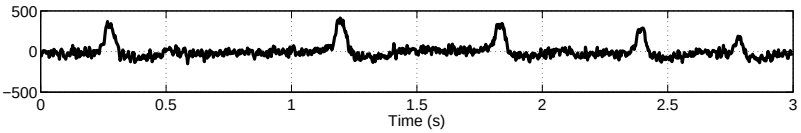

(c) Noisy ECG signal with additive Gaussian white noise at the 10 dB SNR level

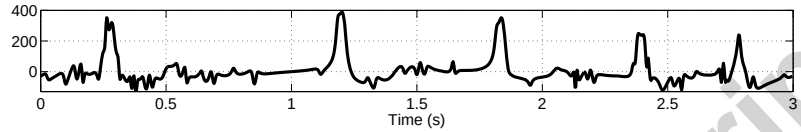

(d) Filtered results using 10 dB as the estimated SNR

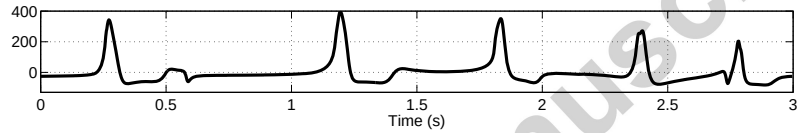

(e) Filtered results using 8.5 dB as the estimated SNR

Figure 9: Comparison between filtered results with different estimated SNRs for the proposed method.

[11] I. Daubechies, J. Lu, H.-T. Wu, Synchrosqueezed wavelet transforms: An empirical mode decomposition-like tool, Appl. Comput. Harmon. Anal. 30 (2) (2011) 243–261. doi:10.1016/j.acha.2010.08.002.

[12] J. P. Amezquita-Sanchez, H. Adeli, Signal processing techniques for vibration-based health monitoring of smart structures, Arch. Comput. Methods Eng. 23 (1) (2016) 1–15. doi:10.1007/s11831-014-9135-7.

[13] M. Das, S. Ari, Analysis of ECG signal denoising method based on S-transform, IRBM 34 (6) (2013) 362–370. doi:10.1016/j.irbm.2013.07.012.

[14] T. Qian, Y. B. Wang, P. Dang, Adaptive decomposition into mono-components, Adv. Adapt. Data Anal. 1 (04) (2009) 703–709. doi:10.1142/S1793536909000278.

[15] R. C. Sharpley, V. Vatchev, Analysis of the intrinsic mode functions, Constr. Approx. 24 (1) (2006) 17–47. doi:10.1007/s00365-005-0603-z.

[16] P. Dang, T. Qian, Y. Y. Guo, Transient time-frequency distribution based on mono-component decompositions, Int. J. Wavelets Multiresolut. Inf. Process. 11 (03) (2013) 1350022. doi:10.1142/S0219691313500227.

[17] T. Qian, Adaptive Fourier decompositions and rational approximations, part I: Theory, Int. J. Wavelets Multiresolut. Inf. Process. 12 (5) (2014) 1461008. doi:10.1142/S0219691314610086.

[18] T. Qian, L. Zhang, H. Li, Mono-components vs IMFs in signal decomposition, Int. J. Wavelets Multiresolut. Inf. Process. 6 (03) (2008) 353–374. doi:10.1142/S0219691308002392.

[19] T. Qian, L. Zhang, Z. Li, Algorithm of adaptive Fourier decomposition, IEEE Trans. Signal Process. 59 (12) (2011) 5899–5906. doi:10.1109/TSP.2011.2168520.

[20] L. Zhang, W. M. W. Hong, T. Qian, Adaptive Fourier decomposition and rational approximation, part II: Software system design and development, Int. J. Wavelets Multiresolut. Inf. Process. 12 (5) (2014) 1461009. doi:10.1142/S0219691314610098.

[21] J. Ma, T. Zhang, M. Dong, A novel ECG data compression method using adaptive Fourier decomposition with security guarantee in e-health applications, IEEE J. Biomed. Health Inform. 19 (3) (2015) 986–994. doi:10.1109/JBHI.2014.2357841.

[22] Z. Wang, C. M. Wong, J. N. da Cruz, F. Wan, P.-I. Mak, P. U. Mak, M. I. Vai, Muscle and electrode motion artifacts reduction in ECG using adaptive Fourier decomposition, in: 2014 IEEE Int. Conf. Syst. Man, Cybern., IEEE, San Diego, CA, USA, 2014, pp. 1456–1461. doi:10.1109/SMC.2014.6974120.

[23] P. E. McSharry, G. D. Clifford, L. Tarassenko, L. Smith, et al., A dynamical model for generating synthetic electrocardiogram signals, IEEE Trans. Biomed. Eng. 50 (3) (2003) 289–294. doi:10.1109/TBME.2003.808805.

[24] G. B. Moody, R. G. Mark, The impact of the MIT-BIH arrhythmia database, IEEE Eng. Med. Biol. Mag. 20 (3) (2001) 45–50. doi:10.1109/51.932724.

[25] A. L. Goldberger, L. A. Amaral, L. Glass, J. M. Hausdorff, P. C. Ivanov, R. G. Mark, J. E. Mietus, G. B. Moody, C. K. Peng, H. E. Stanley, Physiobank, physiotoolkit, and physionet components of a new research resource for complex physiologic signals, Circulation 101 (23) (2000) e215–e220. doi:10.1161/01.CIR.101.23.e215.

[26] V. Marmarelis, Analysis of Physiological Systems: The White-Noise Approach, Springer Science & Business Media, 2012.

[27] T. Pander, A suppression of an impulsive noise in ECG signal processing, in: 26th Annu. Int. Conf. IEEE Eng. Med. Biol. Soc., Vol. 3, IEEE, 2004, pp. 596–599. doi:10.1109/IEMBS.2004.1403228.

[28] T. Qian, L. Tan, Characterizations of mono-components: the blaschke and starlike types, Complex Anal. Oper. Theory (2015) 1–17doi:10.1007/s11785-015-0491-6.

[29] D. Benitez, P. A. Gaydecki, A. Zaidi, A. P. Fitzpatrick, The use of the Hilbert transform in ECG signal analysis, Comput. Biol. Med. 31 (5) (2001) 399–406. doi:10.1016/S0010-4825(01)00009-9.

[30] S. L. Marple, Computing the discrete-time “analytic” signal via

FFT, IEEE Trans. Signal Process. 47 (9) (1999) 2600–2603. doi:10.1109/78.782222.

[31] D. L. Donoho, De-noising by soft-thresholding, IEEE Trans. Inf. Theory 41 (3) (1995) 613–627. doi:10.1109/18.382009.

[32] D. L. Donoho, J. M. Johnstone, Ideal spatial adaptation by wavelet shrinkage, Biometrika 81 (3) (1994) 425–455. doi:10.1093/biomet/81.3.425.

[33] T. Qian, Y. Wang, Remarks on adaptive Fourier decomposition, Int. J. Wavelets Multiresolut. Inf. Process. 11 (1) (2013) 1350007. doi:10.1142/S0219691313500070.

[34] Z. Wang, L. Yang, C. M. Wong, F. Wan, Fast basis searching method of adaptive Fourier decomposition based on Nelder-Mead algorithm for ECG signals, in: Advances in Neural Networks–ISNN 2015, Springer, 2015, pp. 305–314. doi:10.1007/978-3-319-25393-0_34.

[35] J. Pan, W. J. Tompkins, A real-time QRS detection algorithm, IEEE Trans. Biomed. Eng. 32 (3) (1985) 230–236. doi:10.1109/TBME.1985.325532.

[36] Y. Sun, K. Chan, S. Krishnan, Characteristic wave detection in ECG signal using morphological transform, BMC Cardiovasc. Disord. 5 (1) (2005) 28. doi:10.1186/1471-2261-5-28.

[37] M. Kotas, T. Pander, J. M. Leski, Averaging of nonlinearly aligned signal cycles for noise suppression, Biomed. Signal Process. Control 21 (2015) 157–168. doi:10.1016/j.bspc.2015.06.003.

[38] P. Laguna, R. Mark, A. Goldberg, G. Moody, A database for evaluation of algorithms for measurement of QT and other waveform intervals in the ECG, in: Comput. Cardiol. 1997, Vol. 24, IEEE, 1997, pp. 673–676. doi:10.1109/CIC.1997.648140.

[39] J. Martinez, R. Almeida, S. Olmos, A. Rocha, P. Laguna, A wavelet-based ECG delineator: evaluation on standard databases, IEEE Trans. Biomed. Eng. 51 (4) (2004) 570–581. doi:10.1109/TBME.2003.821031.